

Auxiliary material for:

**Choosing a proper complete active space in calculations for
transition metal dimers: Ground state of Mn₂ revisited**

Cristopher Camacho and Henryk A. Witek

Department of Applied Chemistry, National Chiao Tung University,

1001 Ta-Hsueh Road, Hsinchu 30010, Taiwan

Shigeyoshi Yamamoto

Faculty of Liberal Arts, Chukyo University,

101-2 Yagoto-Honmachi, Showa-ku, Nagoya, Aichi 466-8666, Japan

These Auxiliary Materials report additional details of our calculations for the CASSCF and MRMP potential energy curves for the ground state of manganese dimer obtained with a sequence of complete active spaces. First, we present PES of the $^1\Sigma_g^+$ state of Mn_2 calculated using the standard (12o,14e) active space. The problems associated with employing this active space are identified and discussed. Subsequently, we show that augmenting the (12o,14e) active space with a single virtual σ_g orbital is essential for a correct description of the electronic structure of the ground state of Mn_2 . An effect of adding next virtual orbitals to the active space is analyzed and discussed, especially with respect to the change of the shape of PES and the change of the $^1\Sigma_g^+$ wave function. Finally, we investigate the magnitude of the basis set superposition error (BSSE) in our calculations and present counterpoise corrected CASSCF and MRMP potential energy curves and spectroscopic parameters for the $^1\Sigma_g^+$ state.

A. Deficiencies of the (12o,14e) active space

In Figure A we show the calculated CASSCF and MRMP curves for the $^1\Sigma_g^+$ state. The discontinuity point, located approximately at 4.23 Å, is marked with an arrow. The presence of the discontinuity in the CASSCF curve is far from being obvious. The energy difference between the two possible CASSCF solutions is only 10^{-6} hartree, which is comparable with the CASSCF convergence criteria. Also the analytical properties of both possible CASSCF solutions are very similar. The first- and second-order derivatives of the potential energy curve with respect to internuclear separation—given as an inset in Figure A—show that both the solutions are practically indistinguishable. If one concludes the investigation at the CASSCF level, there is a large chance that the discontinuity would remain unnoticed. The disconnected character of both sets of solutions manifests itself very strongly only

after accounting for dynamical correlation; the energy difference at 4.23 Å is as large as 10^{-2} hartree. Below, we analyze this phenomenon in details and discuss the possibility of identifying the discontinuity already at the CASSCF level.

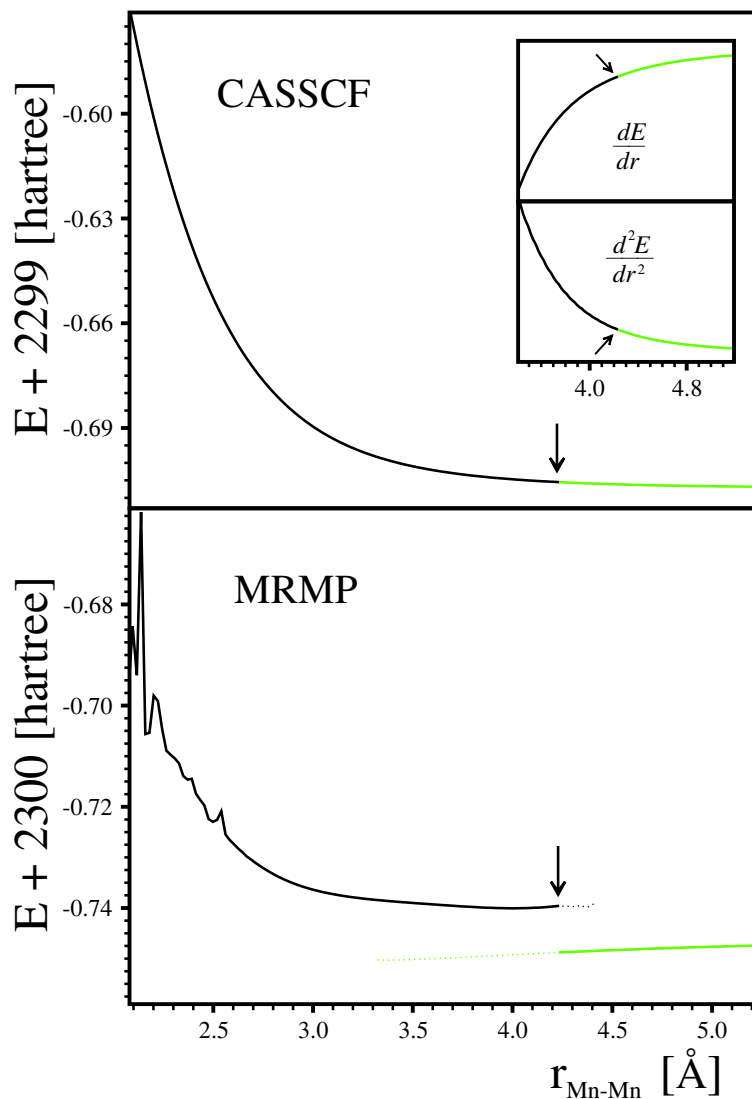


FIG. S1 The CASSCF and MRMP potential energy curves for the $1\Sigma_g^+$ state of Mn_2 calculated using the standard (12o,14e) active space. The black solid lines correspond to stable CASSCF solutions at short internuclear distances. The green solid lines correspond to stable CASSCF solutions at long internuclear distances. Dotted lines correspond to semistable solutions at short and long distances. The inset gives the first and second derivative of the CASSCF potential energy curve.

The discontinuity originates from the coexistence of two stable CASSCF solutions at the

internuclear separation of 4.23 Å. These solutions are also stable (or semistable)¹ in the vicinity of this point. The semistable solutions are plotted in Figures A and B with dotted lines. The main difference between the two solutions stems from a different set of molecular orbitals (MOs) used for constructing the active space. At large internuclear distances, the active orbitals correspond to the σ_g , π_u , δ_g , σ_u , π_g , and δ_u MOs built from the atomic $3d$ and the σ_g and σ_u MOs built from the atomic $4s$ one-electron wave functions. For small internuclear distances, the active orbitals originating from the $3d$ atomic orbitals (AOs) are identical, but the remaining σ_g and σ_u active orbitals are linear combinations of atomic $4s$ and $3p_z$ AOs; the σ_g orbital is dominated by the $4s$ AOs and the σ_u orbital, by the $3p_z$ AOs. The difference between these two stable CASSCF solutions can be described in other words as a difference between interactions of two non-hybridized or sp hybridized atoms. The hybridization occurs abruptly, what can be visualized best by plotting one-electron energies corresponding to the active and doubly-occupied canonical orbitals. They are shown in Figure Ba. We would like to stress that the hybridization discussed here has no physical interpretation; it is a purely mathematical phenomenon that allows for gaining 10^{-6} hartree in CASSCF optimization. In fact, the two σ_g and two σ_u orbitals built from atomic $4s$ and $3p_z$ one-electron wave functions are always doubly occupied, despite of the fact that two of them belong to the active space and two of them, to the doubly-occupied space. This can be seen best from the CASSCF occupation numbers presented in Figure Bb. Simply, the (12o,14e) active space does not permit for creating the $4s+4s$ bond. This is clearly a very good explanation of the previously reported²⁻⁴ repulsive character of the CASSCF curve shown in Figure A.

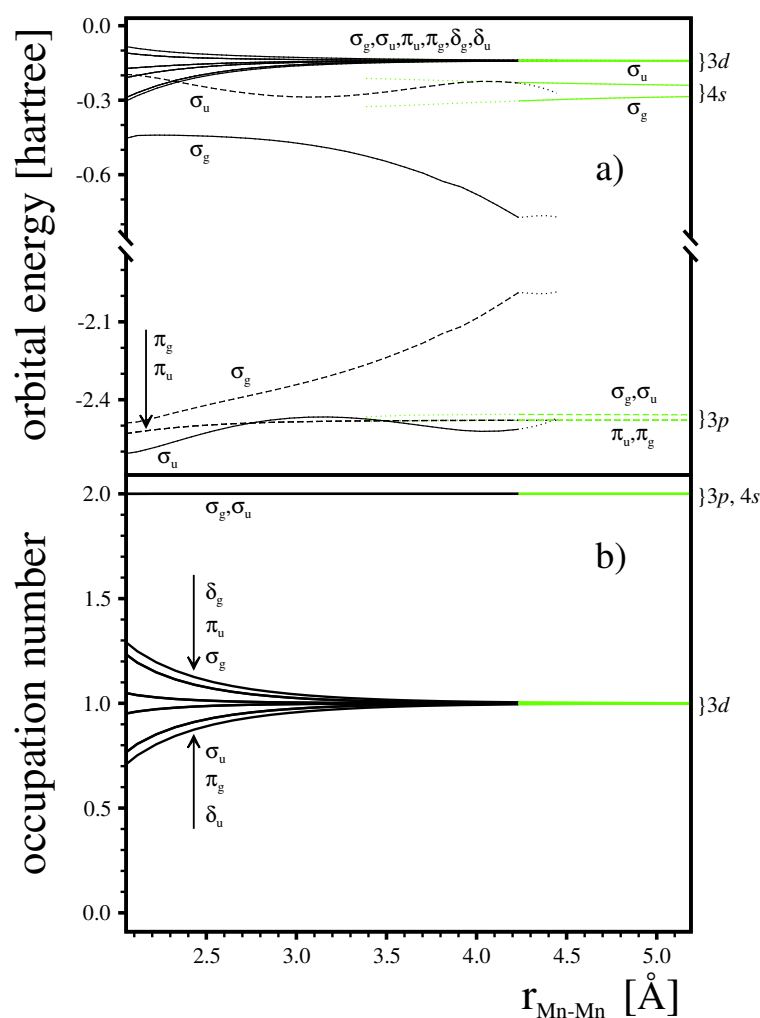


FIG. S2 One-electron Fock energies and occupation numbers of the natural active orbitals calculated for the (12o,14e) complete active space. Lines marked with filled circles correspond to inactive (doubly-occupied) orbitals. For the explanation of colors, see the caption of Figure A.

It is very interesting to note that despite of different MOs used for constructing the active space, the CASSCF wave functions corresponding to both solutions are very similar. Such a situation occurs because in all the important CSFs contributing to the wave functions, the σ_g and σ_u orbitals originating from 4s and from 4s and 3p_z are always doubly occupied. A partial rotation in the hyperplane spanned by two active and two doubly-occupied orbitals

does not, in general, leave the total CASSCF energy invariant. Here, the energy difference corresponding to such a rotation is as small as 10^{-6} hartree only because of effectively closed-shell character of all MOs involved in the rotation. There are a few immediate conclusions arising from these observations.

- The analytical similarity of both CASSCF solutions is readily explained by virtually the same character of the wave functions corresponding to both CASSCF solutions.
- It is rather obvious that the MRMP energies computed using both the active spaces should be different. Clearly, the single and double excitations from and to the active orbitals result in two very different first-order interacting spaces, which give significantly larger differences in energy between the two solutions at the MRMP level. It is also clear that the long-distance solution should be lower in energy since the excitations from the atomic $4s$ orbitals are expected to be more favorable than excitations from the atomic $3p_z$ orbitals.
- One way of avoiding the above mentioned problems with discontinuities in PES is to add an additional virtual σ_g orbital to the active space. This procedure results in a bound ground state of Mn_2 at the CASSCF level. Augmenting the active space with such an orbital would stabilize the correct solution at shorter distances by effective lowering of the occupation number for the σ_u (and possibly σ_g) originating from the atomic $4s$ orbitals.
- Another way of stabilizing the long-distance solution at shorter distances is to perform a state-average CASSCF calculation. The first excited state of the manganese dimer corresponds effectively to a transfer of a single electron from $4s$ into $3d$. A set of MOs averaged over the ground and the first excited states would yield the occupation

numbers smaller than two for the σ_g and σ_u MOs constructed from the atomic $4s$ AOs and would prevent their mixing with doubly occupied orbitals. Similar approach—based on averaging the lowest three A_g states—was used⁴ to determine the previously reported PES for the $^1\Sigma_g^+$ state of Mn_2 . Note, that in many situations state-average orbitals may not guarantee optimal description of the electronic wave function for the ground state and that a state-specific MOs are preferable.

B. PES calculated with an augmented (13o,14e) active space

The CASSCF potential energy curve, shown in Figure 1, is bound with a minimum located at 3.53 Å and with the corresponding harmonic vibrational frequency of 66 cm^{-1} . These values are close to the previously reported^{4,5} theoretical ($r_e=3.29$ Å and $\omega_e=54$ cm^{-1}) and experimental spectroscopic parameters ($r_e=3.4$ Å and $\omega_e=68$ cm^{-1}). The overall shape of the CASSCF PES is similar to the previously published, (12o,14e) MCQDPT potential energy curve computed with stated-average orbitals.⁴ Clearly, the additional σ_g orbital is necessary for a correct description of static correlation in the $^1\Sigma_g^+$ state of Mn_2 . This observation is further justified by the analysis of occupation numbers of the active orbitals given below. It is tempting to state here that the (13o,14e) CASSCF calculations are capable of reproducing accurately the bonding mechanism in Mn_2 . However, a careful study of CASSCF curves obtained with other active spaces shows that the situation is more delicate. Therefore, we restrict ourselves with a further discussion of this issue until later.

It is worth to devote some attention to the analysis of the wave function of the $^1\Sigma_g^+$ state. As mentioned earlier by Bauschlicher², the Mn_2 ground state wave function is highly multiconfigurational. Bauschlicher used a restricted active space comprising a few thousands of CSFs to show that the $^1\Sigma_g^+$ wave function contains 135 CSFs with linear combination

(CI) coefficients larger than 0.05. The CI coefficient corresponding to the closed-shell HF solution was as small as 0.08. The weight of this configuration—computed as a square of the CI coefficient—was as small as 0.6%. This value is spectacularly smaller than 45% obtained⁶ for the HF configuration in the ground state of Cr₂, which is considered to be a representative example of a multiconfigurational wave function. The difference of magnitude between these two values may illustrate the scale of difficulty corresponding to a proper description of the Mn₂ ground state wave function and at the same time explain the complete failure of the density functional theory.⁷⁻⁹ Here, we analyze the $^1\Sigma_g^+$ wave function of Mn₂ in terms of CI coefficients for all the Slater determinants spanning the eight studied complete active spaces. Figure C shows the CI coefficients larger than 0.02 for four of the studied active spaces as a function of internuclear separation. It is very surprising how similar are these curves calculated for different active spaces! All plots in Figure C contain the same number of curves (572) that are separated into four groups resulting from different spin-spin coupling schemes. The group with largest coefficients comprises 32 closed-shell Slater determinants. For all of the plotted Slater determinants, the σ_g orbital originating from the 4s AOs is doubly occupied. The main difference between these determinants stems from different way of distributing the remaining active electrons among the MOs originating from the 3d atomic orbitals. To complete the description of the $^1\Sigma_g^+$ wave function, we present in Figure D the total contribution of the leading 572 Slater determinants to the CASSCF wave function at various distances. The data in Figure D is displayed for the same active spaces that are shown in Figure C. A more detailed analysis of the composition of the total CASSCF wave function is given here explicitly for the (13o,14e) active space at two internuclear separations, at 5.08 Å that corresponds to almost separated atoms and at 3.39 Å, which is very close to the MRMP equilibrium distance. The leading 32 closed-shell Slater determinants contribute only

to 15.7% of the total CASSCF wave function at the equilibrium geometry. The contribution from the leading single Slater determinant is only 0.5%. For the larger distance, the leading Slater determinants constitute the following fraction of the CASSCF wave function: 18.3% for the leading 32 determinants, 59.0% for 192, 68.7% for 252, and 89.1% for 572. For the equilibrium distance, the corresponding numbers are: 15.7% for the leading 32 determinants, 50.7% for 192, 59.1% for 252, and 76.6% for 572. The presented data clearly show that the ground state of Mn_2 is characterized by a truly multiconfigurational wave function. They also explain the failure of single-reference approaches.

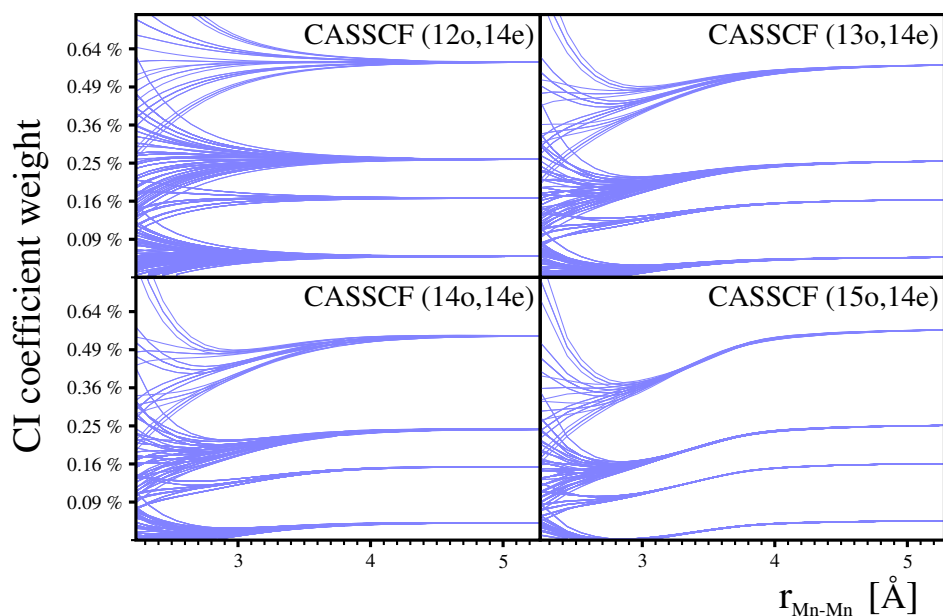


FIG. S3 Weight of the leading Slater determinants as a function of the Mn–Mn distance for the ${}^1\Sigma^+$ CASSCF wave function of manganese dimer. The weights, calculated as squares of the corresponding CI coefficients, are shown for four considered active spaces.

C. Larger active spaces

The CASSCF potential energy curves computed using the (13o,14e), (13o,12e), (12o,12e), and (14o,12e) active spaces are similar to each other. In contrast, the CASSCF curves obtained with the (14o,14e) and (15o,14e) active spaces are very different. The (14o,14e) CASSCF PES is repulsive mainly due to a significantly lower dissociation limit originating from substantial intraatomic correlation. The (15o,14e) CASSCF PES, on the contrary, corresponds to noticeably stronger bond ($\omega_e=120\text{ cm}^{-1}$) with considerably shorter equilibrium distance ($r_e=3.19\text{ \AA}$). It is interesting to note that including auxiliary virtual orbitals in the active space can modify the character of the CASSCF potential energy curve in such a dramatic degree. This example shows that for weakly bound molecules, like Mn_2 , the CASSCF method may give almost arbitrary information about the shape of the ground state potential energy curves owing to a very delicate balance between the bonding and antibonding character of the active orbitals. (Similar effect was observed previously for Cr_2 ^{6,10,11}, Be_2 ¹², and high-spin states of Mn_2 .¹³) This arbitrariness partially vanishes after accounting for dynamical correlation. The calculated MRMP curves have similar characteristic with the exception of the (15o,14e) curve, which we discuss separately below. All of the curves are bound. They have comparable curvature and the minimum located at approximately similar distance. The spectroscopic parameters derived from these curves and given in Table II have similar values like those previously obtained from the MCQDPT calculations.⁴

This positive impression is somewhat depreciated after a closer inspection of the (15o,14e) MRMP curve, which displays a strange feature (a hump) between 2.4 and 3.8 \AA . We believe that the peculiar shape of the (15o,14e) MRMP curve is caused by strong mixing of the two lowest $^1\Sigma_g^+$ wave functions in this region. Such an avoided crossing of these two states

yields the characteristic short equilibrium distance in the (15o,14e) CASSCF calculations and is responsible for the hump in the MRMP curve. The origin of the hump is associated with different amount of dynamical correlation for both the diabatic states. Performing PT calculations for both states and allowing for an interaction of the two perturbed wave functions—as it is done, for example, in the MCQDPT method—would recover the proper shape of the ground state PES. At present, we are not able to perform such calculations owing to serious problems with converging the Davidson eigenvalue algorithm for higher $S_z = 0$ states. Another evidence for the avoided crossing can be obtained from an analysis of Figures C and D, where the distance-dependent composition of the ground state wave functions is given for various active spaces. The CI coefficients for the leading Slater determinants in the (15o,14e) CASSCF wave function are similar to those computed with other active spaces only for short and long interatomic distances. For the intermediate distances, the CI coefficients are noticeably smaller than for the other active spaces. This effect is most clearly visible from Figure D, giving the total contribution from the leading 572 Slater determinants to the CASSCF wave functions. Small CI coefficient in the intermediate region can be readily understood if one assumes strong wave function mixing; an admixture of the first excited state effectively lowers the contribution from other ground state determinants. This finding depletes the common assumption that the large atomic excitation energy for the Mn atom does not permit for effective bonding contributions from the excited atomic terms of manganese.

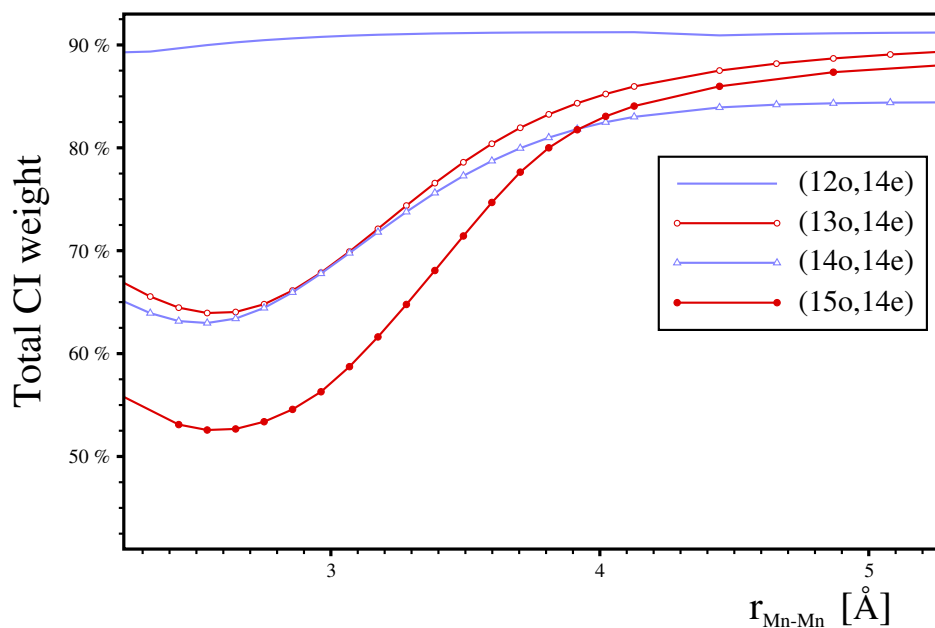


FIG. S4 Total CI weight of the leading 572 Slater determinants as a function of the Mn–Mn distance for the ${}^1\Sigma^+$ CASSCF wave function of manganese dimer. The weights, calculated as the sum of squares of the corresponding CI coefficients, are shown for four considered active spaces.

D. BSSE corrections and non-size consistency error

It is not completely clear how to compute the basis set superposition error (BSSE) corrections for the CASSCF and MRMP calculations in arbitrary active spaces. Here, we adopt the counterpoise correction approach where the valence CASSCF wave function of the single manganese atom has been used as the reference function and the energy is computed as a function of the separation of the auxiliary basis set. Most of the active spaces considered by us in this study possess an asymmetric character owing to the lack of balance between the bonding and antibonding molecular orbitals. Usually, active spaces in CASSCF calculations for dimers are symmetric, i.e., they dissociate to identical atomic active spaces. Some of the active spaces considered here are “asymmetric”, i.e., they give not identical

atomic active spaces upon dissociation. It is difficult to transfer this asymmetric character directly to atomic calculations. We have decided to perform the counterpoise corrections to the CASSCF and MRMP energies for the 6S ground state of the Mn atom using the full (9o,7e) and the reduced (6o,7e) valence atomic active spaces. Note that the “asymmetric” molecular active spaces employed by us for Mn_2 are intermediate between these two limiting atomic cases, (6o,7e)+(6o,7e) and (9o,7e)+(9o,7e). The BSSE corrections computed for both limiting cases have similar magnitude. The BSSE correction energies are consistently larger for the full valence active space; we have decided to use the full valence active space BSSE to determine the counterpoise corrections for the CASSCF and MRMP curves. The magnitude of BSSE is shown in Figure E separately for CASSCF (upper panel) and MRMP (lower panel). The BSSE corrections at the CASSCF level are small. The counterpoise corrected CASSCF potential energy curves are almost identical to the original ones. The corrections at the MRMP level are approximately thirty times larger than for CASSCF. An example of PES calculated using the CASSCF and MRMP methods with and without the BSSE corrections is shown in Figure F for the (13o,14e) active space. The MRMP curves with the BSSE corrections in general have more shallow potential energy wells with minima shifted toward longer distances.

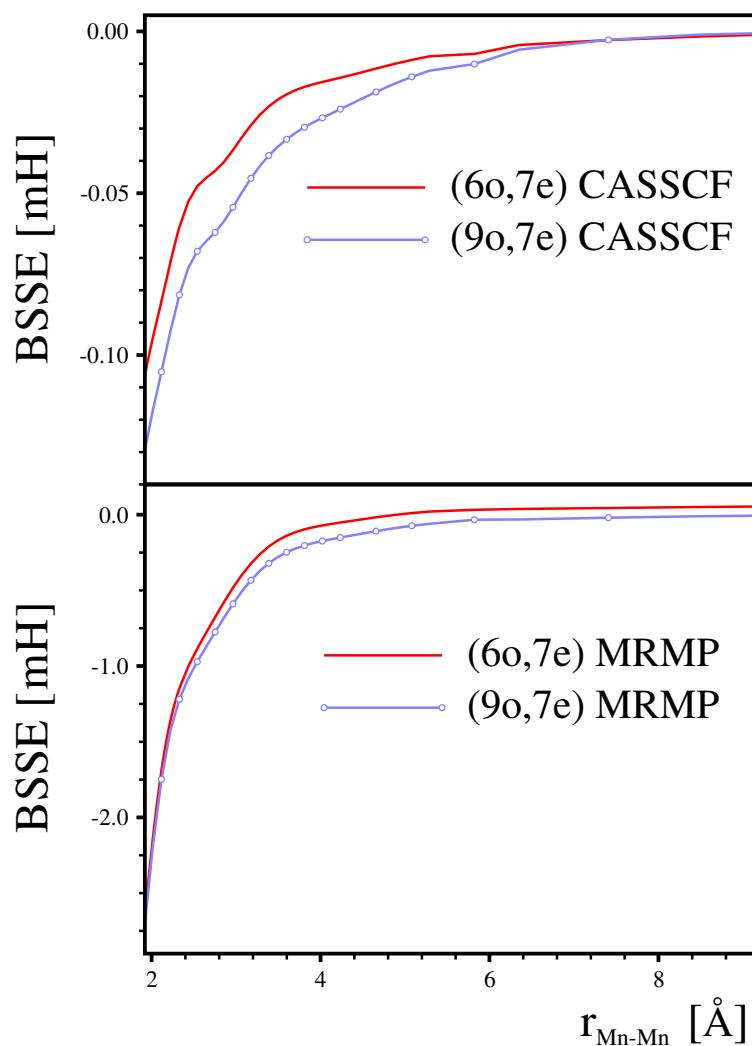


FIG. S5 The magnitude of the distance-dependent BSSE corrections for the atomic reduced-valence (6o,7e) and full-valence (9o,7e) active space calculated with the CASSCF (upper panel) and MRMP (lower panel) methods.

It is well known that the second-order multireference perturbation theory can display large non-size consistency errors. We have performed the size consistency test for the manganese dimer using the reduced (6o,7e) atomic CAS. The computed MRMP energy of two atoms separated by 95 Å is -2300.7470107021 hartree. The doubled MRMP energy of a single Mn atom is -2300.7471303034. Therefore, in our case, the non-size consistency error is small; it is only 10^{-4} hartree. However, we have discovered another interesting peculiarity

of the MRMP method, namely that the MRMP atomic energy depends strongly on the auxiliary basis sets centered on some ghost atom, even if this basis set is located at infinite separation! The MRMP energy of a single Mn atom is -1150.3735651517 hartree and the MRMP energy of a single atom calculated using the auxiliary basis set located 95 Å away is -1150.3550868532 hartree. The later energy is 0.0185 hartree *higher*, which is completely counterintuitive. To confirm this finding, we have introduced a third basis set located also 95 Å away from the atom and 190 Å away from the first auxiliary basis set. This change has resulted in another energy rise, by 0.0210 hartree, to the value of -1150.3341382656 hartree. To verify the validity of this analysis, we have compared the CASSCF energies in these three calculations. They are identical and equal to -1149.853545805 hartree. No plausible explanation can be given for the observed MRMP peculiarity. Clearly, this phenomenon is related neither to lack of size-consistency nor to lack of size-extensivity, since we have only a single atom and a constant number of electrons in our calculations. It is also not related to symmetry-breaking in the MRMP calculations, since the single atom calculations use the D_{2h} point group, while the augmented calculations use the C_{2v} and D_{2h} points groups, respectively. Therefore, we have decided to present detailed numerical values obtained from our calculations to facilitate other researchers to reproduce these results. It is important to state that this phenomenon is observed only for the reduced valence active space. For the full valence CAS, the energy rise upon introducing an auxiliary basis set is smaller than 10^{-8} hartree. Note that the discussed MRMP peculiarity is responsible for elevation of the (6o,7e) BSSE curve in Figure E in comparison with the (9o,7e) BSSE curve.

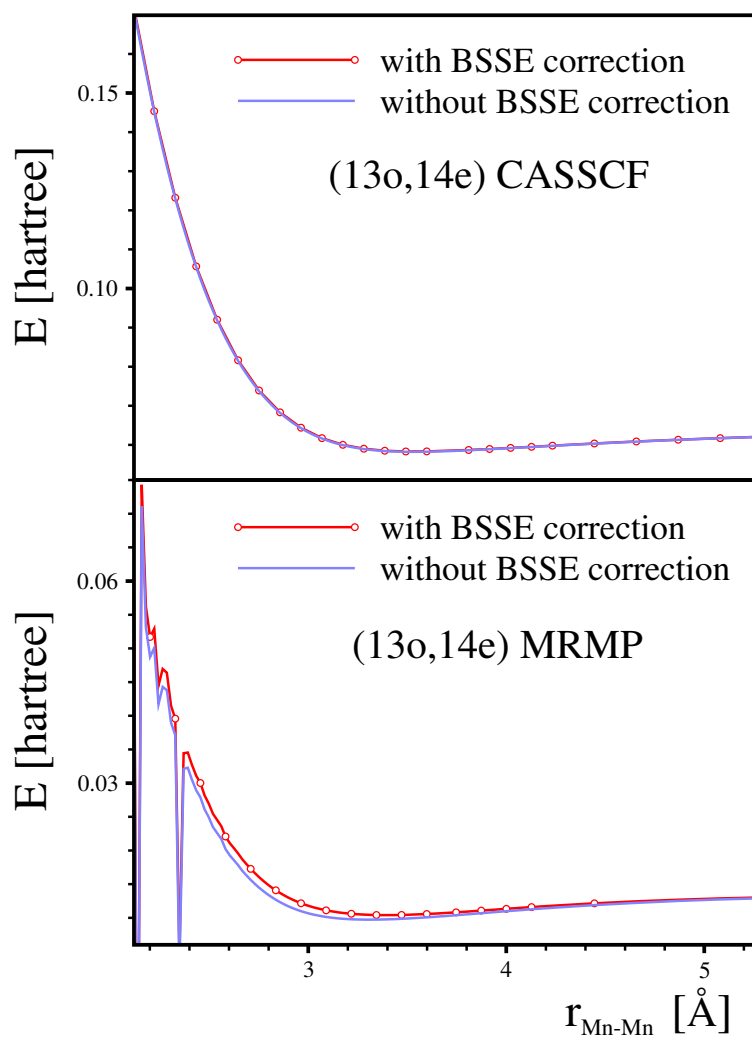


FIG. S6 The (13o,14e) CASSCF and MRMP potential energy curves for the ground state of Mn_2 calculated with and without the BSSE corrections

E. How short can be the bond in Mn_2 ?

We would like to signalize here the possibility of significant shortening of the equilibrium distance in Mn_2 owing to a strong admixture of Slater determinants originating from the $4s^13d^6 + 4s^13d^6$ or $4s^13d^6 + 4s^23d^5$ atomic dissociation limits. One may say that there is no evidence for such shortening, neither experimental nor theoretical, and that our theo-

retical results seem to confirm the validity of existing experimental data. Moreover, the atomic ${}^6S \rightarrow {}^6D$ promotion energy¹⁴ is as high as 2.14 eV, which prevents effective mixing of such determinants due to large energetic separation. However, the CASSCF calculations performed with the (15o,14e) active space have revealed—as discussed above—that between 2.4 and 3.8 Å the energy separation between these two groups of determinants is rather small and they can strongly mix causing additional energy lowering and leading to a short-distance minimum. The shape of the (15o,14e) MRMP curve, indicating that the amount of dynamic correlation contribution to both groups of determinants is different, suggests that the Slater determinants originating from the $4s^23d^5 + 4s^23d^5$ atomic limit are stabilized in a larger degree. Nevertheless, we believe that large active space, multistate multiconfigurational perturbation study of low-lying states of Mn_2 , in which the states would be allowed to interact also *after* accounting for dynamical correlation via the effective Hamiltonian formalism, could possibly produce PES with a short-distance minimum. Here, we feel it is necessary to communicate this possibility in hopes that somebody can address this issue in the future using the multistate formalism.

F. ORMAS estimation of the full-valence CASSCF PES

The curves obtained using the largest considered active spaces, i.e. the (14o,14e) MRMP curve and the (15o,14e) CASSCF curve, have their minima at shorter distances than the curves calculated with smaller active spaces. Would the equilibrium distance be even shorter if one employs larger active spaces? Is it possible—judging from the gradual change of the CASSCF potential energy curve with the growing size of CAS—that the CASSCF potential energy surface computed with the full valence active space would have a minimum at approximately 3.0 Å? Or would it be rather repulsive, similarly to the (14o,14e) CASSCF curve,

owing to significantly lower atomic dissociation limit? Unfortunately, at present, complete active space SCF calculations using larger active spaces are beyond our reach and we have to leave these questions unanswered. However, we can try to anticipate the shape of the full valence space SCF curve for the ground state of Mn_2 using some restricted active spaces. For this purpose, we perform our SCF calculations using the occupation-restricted multiple active spaces (ORMAS) approach^{15,16} implemented in the GAMESS package.¹⁷ Three different ORMAS schemes are tested. In the first scheme, we partition the full valence active space of Mn_2 as a product of two CAS subspaces: (10o,10e) corresponding to the atomic $3d$ orbitals and (8o,4e) corresponding to the atomic $4s$ and $4p$ orbitals. This choice is motivated by the chemically inactive character of the $3d$ orbitals deduced from Figure 2; the composite occupation number of these orbitals is very close to 10 over the whole PES. In the second scheme, the full valence active space of Mn_2 is divided into three CAS symmetry subspaces: (6o,6e), (8o,4e), and (4o,4e) corresponding to the σ , π , and δ MOs, respectively. In the third approach, we divide active MOs into three groups that correspond to atomic $4s$, $3d$, and $4p$ orbitals; the $3d$ subspace contains 10 electrons, the $4s$ subspace can contain 2, 3, or 4 electrons, and the $4p$ subspace can contain 0, 1, or 2 electrons. The MCSCF curves obtained using these three schemes are shown in Figure G. Unfortunately for the second approach, only the long-distance ORMAS SCF calculations converge showing that dividing the active orbitals into the σ , π , and δ subspaces is not justified chemically. Both of remaining two curves are repulsive; they have similar shape to the CASSCF PESs obtained with the (12o,14e) and (14o,14e) active spaces. The results obtained with loosened SCF convergence criterion for the second approach show similar regularities. These findings suggest that the full valence (18o,14e) CASSCF curve is indeed repulsive and that the bound character of the ground state of Mn_2 is recovered only after accounting for dynamical correlation. To

verify the accuracy of the ORMAS approach used by us to predict the shape of the full valence PES, we have performed a test of ORMAS for the (13o,14e) active space, for which the exact CASSCF solutions are known. Namely, we have performed the SCF calculations using two ORMAS schemes: $(10o,10e) \otimes (3o,4e)$ and $(5o,6e) \otimes (4o,4e) \otimes (4o,4e)$, obtained in an analogous way to that one described above. Both these ORMAS curves (shown in Figures H and I) are practically indistinguishable from the (13o,14e) CASSCF potential energy surface. This test—being of course far from a formal evidence—gives us a strong trace that the ORMAS estimations of the full valence active space potential are accurate and that the (18o,14e) CASSCF curve is indeed repulsive. Another way of addressing this issue is employing restricted active space¹⁸ or quasi-complete active space¹⁹ SCF formalisms followed by appropriate perturbation calculations. A theoretical study using these methods would definitely help to shed some more light on the issues discussed above.

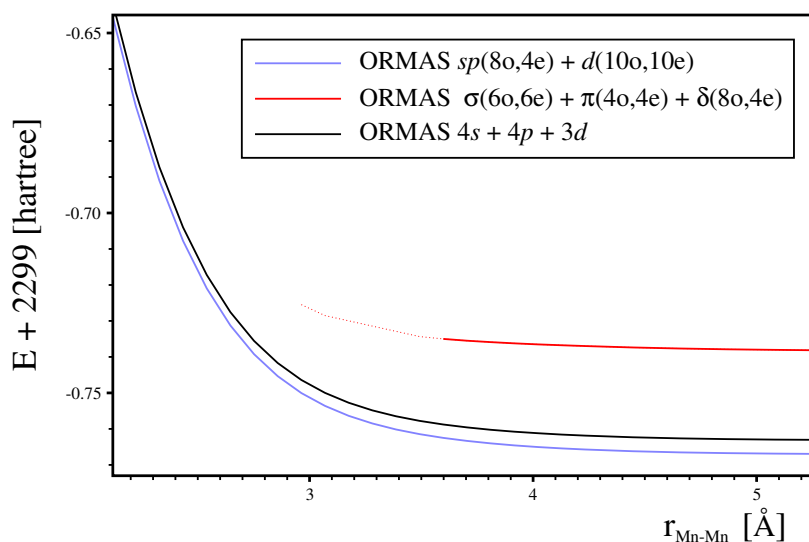


FIG. S7 Estimates of the full-valence (18o,14e) CASSCF potential energy curve obtained using three different ORMAS schemes, $d(10o,10e) \otimes sp(8o,4e)$, $\sigma(6o,6e) \otimes \pi(8o,4e) \otimes \delta(4o,4e)$, and $d(10o,10e) \oplus s(2o,3e) \otimes d(10o,10e) \otimes p(6o,1e) \oplus s(2o,2e) \otimes d(10o,10e) \otimes p(6o,2e)$. For details, see text.

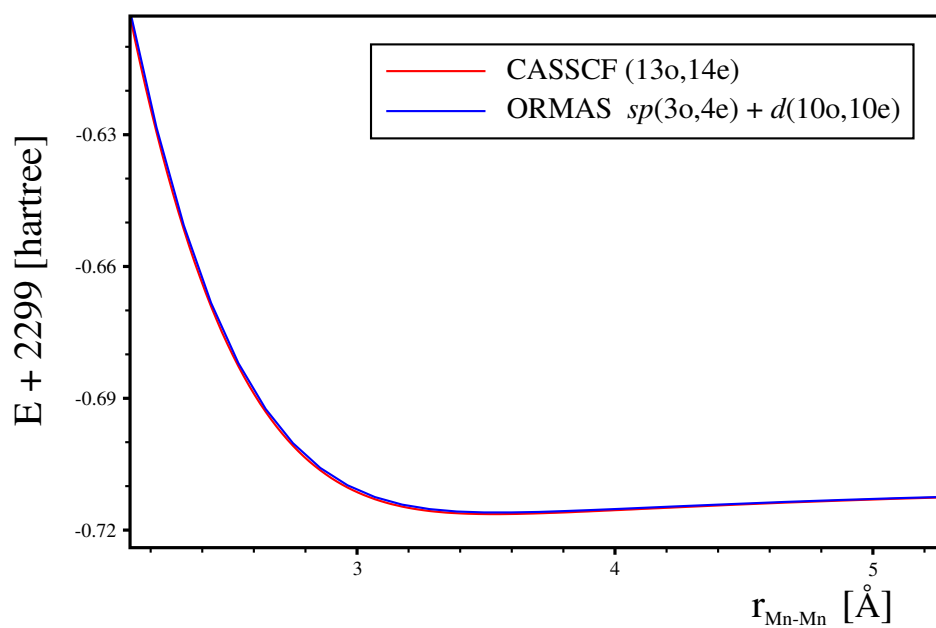


FIG. S8 Estimate of the (13o,14e) CASSCF potential energy curve obtained using the $d(10o,10e) \otimes sp(3o,4e)$ ORMAS scheme.

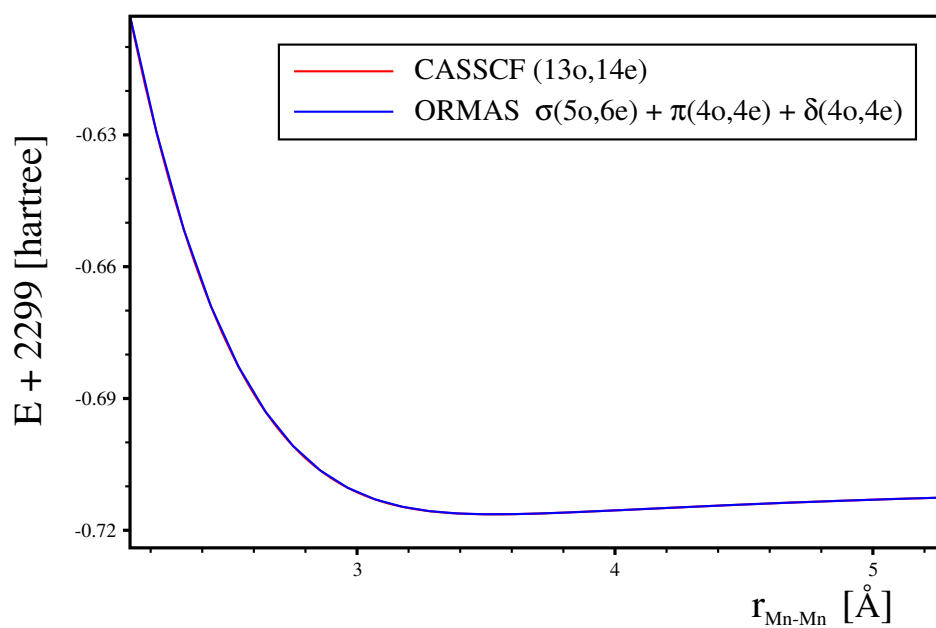


FIG. S9 Estimate of the (13o,14e) CASSCF potential energy curve obtained using the $\sigma(5o,6e) \otimes \pi(4o,4e) \otimes \delta(4o,4e)$ ORMAS scheme.

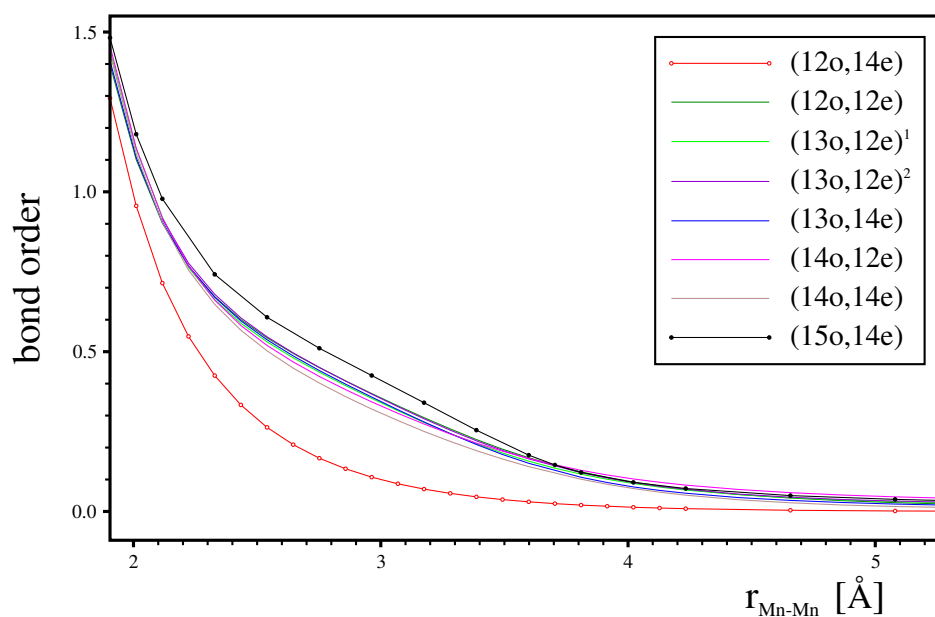


FIG. S10 Bond order as a function of the Mn–Mn distance for the eight active spaces studied.

-
- ¹ Semistable solution denotes a solution obtained with loosened SCF convergence criterion. Note that since our calculations use very tight SCF criteria, in some case our "loosened convergence criteria" may be even more rigorous than the program defaults.
- ² C. W. Bauschlicher, Jr., *Chem. Phys. Lett.* **156**, 95 (1989).
- ³ B. Wang and Z. Chen, *Chem. Phys. Lett.* **387**, 395 (2004).
- ⁴ S. Yamamoto, H. Tatewaki, H. Moriyama, and H. Nakano, *J. Chem. Phys.* **124**, 124302 (2006).
- ⁵ A. D. Kirkwood, K. D. Bier, J. K. Thompson, T. L. Haslett, A. S. Huber, and M. Moskovits, *J. Phys. Chem.* **95**, 2644 (1991).
- ⁶ B. O. Roos, *Collect. Czech. Chem. Commun.* **68**, 265 (2003).
- ⁷ S. K. Nayak and P. Jena, *Chem. Phys. Lett.* **289**, 473 (1998).
- ⁸ S. Yanagisawa, T. Tsuneda, and K. Hirao, *J. Chem. Phys.* **112**, 545 (2000).

- ⁹ S. Yamanaka, T. Ukai, K. Nakata, R. Takeda, M. Shoji, T. Kawakami, T. Takada, and K. Yamaguchi, *Int. J. Quant. Chem.* **107**, 3178 (2007).
- ¹⁰ B. O. Roos and K. Andersson, *Chem. Phys. Lett.* **245**, 215 (1995).
- ¹¹ B. O. Roos, *Acc. Chem. Res.* **32**, 137 (1999).
- ¹² J. Martin, *Chem. Phys. Lett.* **303**, 399 (1999).
- ¹³ A. A. Buchachenko, private communication.
- ¹⁴ J. Sugar and C. Corliss, *J. Phys. Chem. Ref. Data* **14**, Suppl. 2 (1985).
- ¹⁵ J. Ivanic, *J. Chem. Phys.* **119**, 9364 (2003).
- ¹⁶ J. Ivanic, *J. Chem. Phys.* **119**, 9377 (2003).
- ¹⁷ M. W. Schmidt, K. K. Baldridge, J. A. Boatz, S. T. Elbert, M. S. Gordon, J. H. Jensen, S. Koseki, N. Matsunaga, K. A. Nguyen, S. Su, et al., *J. Comput. Chem.* **14**, 1347 (1993).
- ¹⁸ J. Olsen, B. O. Roos, P. Jørgensen, and H. Jensen, *J. Chem. Phys.* **89**, 2185 (1988).
- ¹⁹ H. Nakano, J. Nakatani, and K. Hirao, *J. Chem. Phys.* **114**, 1133 (2001).